Available online at www.sciencedirect.com

ScienceDirect

Energy Procedia 8 (2011) 515–520

Energy Procedia

1st International Conference on Silicon Photovoltaics

Efficiency Improvement by Deeper Emitter with Lower Sheet Resistance for Uniform Emitters

Y. Komatsu[a]*, M. Koorn[a], A.H.G. Vlooswijk[b], P.R. Venema[b], A.F. Stassen[a]

[a]*ECN Solar Energy,P.O.Box 1, 1755ZG Petten, the Netherlands*
[b]*Tempress Systems BV, Radeweg 31, 8171MD Vaassen, the Netherlands*

Abstract

By reducing the peak concentration of phosphorus doping and raising the sheet resistance of a uniform emitter from 66 to 76 ohm/square, a 0.2%$_{abs}$ efficiency gain was achieved for multicrystalline silicon solar cells. No extra process time or step is needed to obtain this improved efficiency. Increasing the sheet resistance and reducing the peak concentration narrows the process window. Manipulation of the doping profile towards a deeper emitter with lower peak concentration does not have these drawbacks. The resulting process leads to a 0.3%$_{abs}$ efficiency gain at a lower sheet resistance (51-56 ohm/square). A wide process window with a large tolerance for metal contacting is obtained. By statistical analysis and PC1D simulations, the legitimacy of the positive contribution of the deeper emitter is shown.

Keywords: phosphorus diffusion; uniform emitter; doping profile; sheet resistance; contact resistance; process window; PC1D

1. Introduction

The dominant part of the crystalline silicon solar cell market consists of products with uniform emitters. This situation will continue for some time being due to the simple and proven production process. A proven concept prefers refinements of a single process step to replacing process steps or adding extra steps.

Uniform emitter processes have undergone such refinements for decades. With development of fire-through Ag contact paste, emitter depth became shallower and sheet resistance (R_{sheet}) increased. By

* Corresponding author. Tel.: +31-224-56-4761; fax: +31-224-56-8214.
E-mail address: komatsu@ecn.nl.

1876–6102 © 2011 Published by Elsevier Ltd. Selection and/or peer-review under responsibility of SiliconPV 2011.
doi:10.1016/j.egypro.2011.06.175

increasing control of the penetration depth of Ag paste and improved uniformity of the diffusion process, the process window has been narrower and the average R_{sheet} as the center point of the window has been increased; higher R_{sheet} contributes to improvement of short circuit current (I_{sc}) and open circuit voltage (V_{oc}), but the gain in output power is limited by a loss in fill factor (FF) over a certain R_{sheet}.

Emitters made by phosphorus diffusion consist of two distinct layers both heavily doped: a so-called n^{++} layer close to the surface; and a slightly lighter doped n^{+} layer underneath. Bentzen et al. clarified the unique feature of phosphorus diffusion into silicon [1], which explains that the border of the n^{++} and the n^{+} layers always appears where the phosphorus concentration (N_P) is ~3×10^{19} /cm³, due to the 5-7 times larger diffusivity of phosphorus (D_P) at $N_P = 1\times10^{19}$ /cm³ than D_P at $N_P = 1\times10^{20}$ /cm³.

The increase in R_{sheet} contributes to the improvement of both I_{sc} and V_{oc} by reducing the density of carrier recombination centers. Especially in the n^{++} layer where $N_P > 1\times10^{20}$ /cm³, the bandgap narrowing effect is significant [2] and the impact of Auger recombination is too large to ignore [3]. The excess phosphorus above 5×10^{20} /cm³ is electrically inactive [4], causing Shockley-Read-Hall (SRH) recombination [5]. Our previous work [4] focused on reducing these SRH recombination centers by decreasing the peak N_P of the n^{++} layer from 2×10^{21} /cm³ to 5-8×10^{20} /cm³, while keeping R_{sheet} 60-70 ohm/square. This resulted in a $0.2\%_{abs}$ efficiency gain. By further manipulation of the phosphorus doping profile [6] while keeping the total process duration constant, an efficiency gain of 0.2-$0.3\%_{abs}$ has been achieved. This has been obtained with a R_{sheet} of 47-57 ohm/square, over 10 ohm/square lower than the reference emitter. In that work, we showed that not only the lower peak N_P in the n^{++} layer but also the deeper n^{+} layer contributes to the efficiency gain. Since then, merely characterizing the emitter as "high sheet resistance" or "shallow emitter" has no longer been indicative for high efficiency.

In this work, we further analyze the cause of the efficiency improvement, and indicate the direction to optimize the emitter doping profile towards wider process window as well as higher efficiency.

2. Experiment

An industry-scale $POCl_3$ tube furnace Tempress TS81003, equipped with 400 slots for loading 156×156 mm² wafers in its temperature flat zone was used for diffusion. We implemented a steam generator RASIRC® Steamer 125 [6] to the $POCl_3$ furnace in order to manipulate the doping profile. The doping profiles were characterized with secondary ion mass spectroscopy (SIMS).

21 groups of different phosphorus diffusion processes were tested including the reference group with the conventional process currently used by the industry. The total process times of all groups are comparable. A process with the highest average R_{sheet} (7×7 points in a wafer) was selected to optimize the Ag paste process so as to achieve the highest FF.

Polished CZ Si wafers out of a single lot were used for characterizing the doping profiles. 156×156 mm² multicrystalline silicon (mc-Si) wafers were used for manufacturing solar cells whose process is almost identical to industrial production process except in the degree of automation. Except for the phosphorus diffusion process, all other process steps —like texturing; SiN_x deposition; Ag paste; etc.— were the identical for all samples and processed in one time to the utmost. Neighboring wafers were equally distributed to each group whose size was 10-12 completed cells. More details are described in [6].

3. Results

3.1. Reducing the peak of n^{++} layer

In Fig.1, the doping profile of the reference group with an average R_{sheet} of 66 ohm/square is displayed, accompanied by two other doping profiles with 76 and 85 ohm/square, respectively. The processes for

these profiles were designed with the consideration to reduce the peak N_P of the n^{++} layer while keeping the profile of the n^+ layer intact. The n^+ profiles of both the red and the blue curves exactly coincide with the reference black curve while peak concentrations N_P are reduced significantly and the n^{++} layer depths are reduced. Both lower peak and shallower depth of the n^{++} resulted in higher sheet resistance.

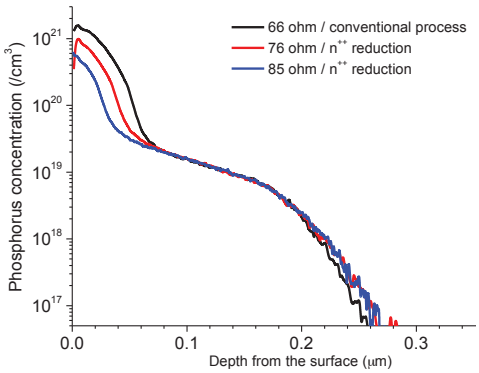

Fig. 1. Phosphorus doping profiles of reference (conventional process) 66 ohm/sq., n^{++}-reduced 76 ohm/sq., and 85 ohm/sq. groups.

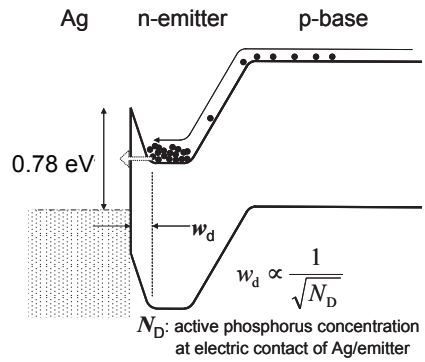

Fig. 2. Band diagram of Ag contact / n-emitter / p-base while illuminated. Electrons at n-emitter travel to Ag contact as a tunneling current through the space charge layer with a thickness w_d.

Table 1. Average values with standard deviations of J_{sc}, V_{oc}, FF, efficiency and R_{se} of 10-12 mc-Si solar cells with different doping profiles designed under different considerations with the indication of average R_{sheet} of a wafer out of each group.

R_{sheet} (ohm/square)	J_{sc} (mA/cm²)	V_{oc} (mV)	FF (%)	efficiency (%)	R_{se} (ohm·cm²)	Process design
66.2 ± 1.9	34.4 ± 0.2	612 ± 1	77.6 ± 0.1	16.3 ± 0.1	1.36 ± 0.23	Conventional (Ref)
75.6 ± 4.2	34.8 ± 0.2	618 ± 1	77.0 ± 0.4	16.5 ± 0.1	1.38 ± 0.06	Reduction n^{++}
85.0 ± 1.7	35.2 ± 0.1	621 ± 1	72.8 ± 0.8	15.9 ± 0.2	2.05 ± 0.43	Reduction n^{++}
51.3 ± 2.5	34.5 ± 0.1	617 ± 1	77.9 ± 0.2	16.6 ± 0.1	1.43 ± 0.26	Deepening n^+
55.6 ± 1.3	34.6 ± 0.2	619 ± 1	77.6 ± 0.2	16.6 ± 0.1	1.46 ± 0.31	Deepening n^+
38.6 ± 1.8	33.9 ± 0.1	616 ± 1	78.4 ± 0.2	16.4 ± 0.1	1.21 ± 0.15	Deepening n^+

The results of manufacturing mc-Si solar cells using the profiles depicted in Fig.1 are shown as the average values with the standard deviations in the top three rows of Table 1. Series resistance (R_{se}) values are calculated from the inclination of the I-V curves at $V = V_{oc}$. The improvement of J_{sc} (short circuit current density) and V_{oc} of both 76 and 85 ohm/sq. cells compared to the reference 66 ohm/sq. suggests that the recombination centers in the n^{++} layer are reduced effectively by means of the lower peak and the shallower layer. The average efficiency gain of the 76 ohm/sq. cells was $0.2\%_{abs}$.

The FF of 85 ohm/sq. cells went down remarkably while the decrease for 76 ohm/sq. cells was limited. The same trend is seen in the difference of R_{se}. The electric contact point between the contact Ag and the emitter should be around 25-50 nm from the surface, according to the reported penetration depth of fire-through Ag paste [7]. A Schottky junction is formed because the impurity level of Ag to conduct electron is 0.78 eV below the conduction level of silicon [5]. The electrons travel from the emitter to the Ag contact as a tunneling current through the space charge layer with a thickness of w_d as shown in Fig. 2. The tunneling probability is almost 100% at the short circuit point, but decreases near the maximum power point of the solar cell operation with the decreasing bias electric field added at the space charge

layer, appearing as the contact resistance. The tunneling probability will decrease faster when w_d is thicker. Because w_d is in inverse proportion to the square root of the active phosphorus concentration (N_D) [5], the 85 ohm/sq. cells (Fig. 1: blue) with lower N_D at 25-50 nm have a lower *FF* with a higher R_{se} where the 76 (Fig. 1: red) and the 66 (Fig. 1: black) ohm/sq. cells with comparable N_D —because it cannot be higher than 5×10^{20} /cm³ [4]— at 25-50 nm have a similar *FF* and R_{se}.

The process tuning direction towards the red curve in Fig. 1 (76 ohm/sq. cells) looks promising, but the process window to reconcile less carrier recombination and lower contact resistance is narrower, considering the steep decrease in N_P at 25-50 nm.

3.2. Deepening n^+ layer

In order to render a wider process window than in the previous section, we designed a diffusion process resulting in a lower peak N_P of the n^{++} layer, combined with a deeper n^+ layer. Figure 3 shows the representative 3 curves of 51 ohm/sq. (dark green), 56 ohm.sq. (pink), and 39 ohm/sq. (dark yellow), showing together with the profiles of Fig.1 for comparison. All three show deeper n^+ layers than the reference black curve, resulting in a lower R_{sheet}. The impact of the lower peak concentration is limited because most of the reduced phosphorus in the n^{++} layer is electrically inactive.

The results of the mc-Si solar cells are shown in the bottom three rows of Table 1. The 51 ohm/sq. cells (Fig. 3: dark green) show higher V_{oc} and *FF*, resulting in 0.3%$_{abs}$ average efficiency gain. The peak N_P is comparable to that of the red curve (76 ohm/sq.), but the n^{++} and n^+ layers are deeper. The region where N_P is no longer above 5×10^{20} /cm³ lies much deeper than the emitters described in section 3.1, rendering a wider process window for the Ag paste to penetrate.

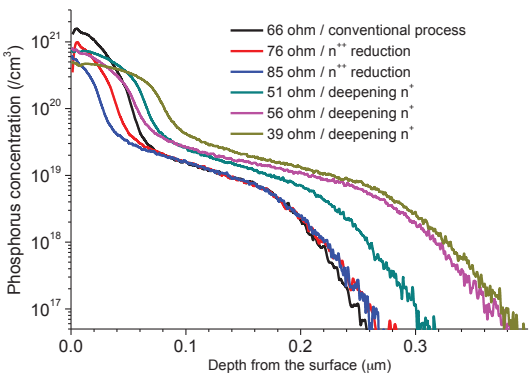

Fig. 3. Phosphorus doping profiles of deepened-n^+ 51 ohm/sq., 56 ohm/sq., and 39 ohm/sq. groups, shown together with the profiles of Fig.1 for comparison.

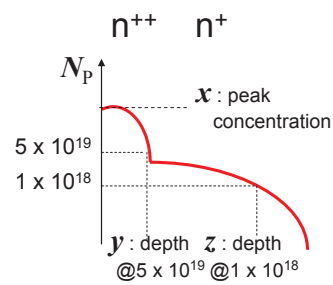

Fig. 4. Simplified model of phosphorus doping profile formed by diffusion process. Variables *x*, *y*, and *z* are also indicated.

The 56 ohm/sq. cells (Fig. 3: pink) show an increase in both J_{sc} and higher V_{oc} compared to the 51 ohm/sq. cells, but despite a lower *FF,* they also result in a comparable 0.3%$_{abs}$ average efficiency gain. The depth tolerance where $N_P > 5\times10^{20}$ /cm³ is narrower than the 51 ohm/sq. cells (Fig. 3: dark green), but wider than the 76 ohm/sq. cells (Fig. 3: red), explains a *FF* more comparable to the reference than to the 76 ohm/sq. cells.

A surprising result is the increase of 7 mV in V_{oc} with such a deep n^+ layer compared to the reference. In general, the concentration of equilibrium minority carrier (hole in this case) decreases with increasing N_D, and the equilibrium hole concentration limits the dark saturation current of the emitter (I_{0e}) [5]. So

far with a more heavily doped n^{++} layer where $N_P > N_D$, the effect of high N_D limiting I_{0e} was hardly observed because of the impact of SRH recombination. This effect is visible due to the successful suppression of SRH recombination in the n^{++}. The equilibrium hole concentration is relatively low at $N_D = N_P = \sim 3\times10^{19}$ /cm³ where the impact of Auger recombination is much smaller than that in the n^{++} layer [3], so the region of $1\times10^{19} < N_P < 3\times10^{19}$ /cm³ with a wide range (~150 nm) of the pink curve in Fig. 3 should cause a reduction in I_{0e} resulting in higher V_{oc}.

In the 39 ohm/sq. cells (Fig. 3: dark yellow) the highest *FF* is observed. The peak N_P is even lower than for the 85 ohm/sq. cells (Fig. 3: blue); the depth tolerance as wide as 60 nm with $N_P > 3\times10^{20}$ /cm³ enables lower contact resistance as indicated in Table 1. But the too deep n^{++} causes reduction in both J_{sc} and V_{oc} due to the increase in the total number of Auger recombination centers under the illuminated region. Even though, V_{oc} is still higher than the reference presumably because of the contribution of the deep n^+ layer, especially the part where $1\times10^{19} < N_P < 3\times10^{19}$ /cm³.

4. Discussion

The contribution of the deeper n^+ is further analyzed. In our previous study [6], the doping profile curve was numerically correlated to the mc-Si solar cell performance using statistical analysis. In this study, we compare the outcome of the analysis with the PC1D simulator [8].

To carry out the numerical analysis, three variables were used: x as peak N_P; y as depth at $N_P = 5\times10^{19}$ /cm³; and z as depth at $N_P = 1\times10^{18}$ /cm³, as a quick numerical expression of the doping profile as indicated in Fig. 4. Variables x and y represent the peak and the depth of the n^{++} layer, respectively, and z represents the depth of the n^+ layer. All individual solar cells of the 21 groups were statistically analyzed with a linear regression model expressed with the next equation:

$$W = \beta_0 + \beta_1 x + \beta_2 y + \beta_3 z + \varepsilon ,$$

where, W is either of J_{sc}, V_{oc}, or *FF*; β_n are statistically estimated coefficients; and ε is the residual error. Further procedure detail and results of the analysis are described in [6].

Using the parameters β_n estimated from the multiple regressions, while keeping x and y constant, the trends of J_{sc}, V_{oc}, and *FF* as a dependence on z can be drawn with comparing the results of the PC1D simulation as shown in Fig. 5. In this comparison, we employed $x = 7.8\times10^{20}$ /cm³ and $y = 0.076$ µm, taken from the 51 ohm/sq. cell (Fig. 3: dark green).

Fig. 5(a) shows the trend of R_{sheet} and *FF* without any PC1D output because PC1D cannot evaluate the factor of lateral conductivity. A deeper n^+ will lead to lower R_{sheet} because of increasing lateral conductivity. With an identical cell design, *FF* will also increases accordingly.

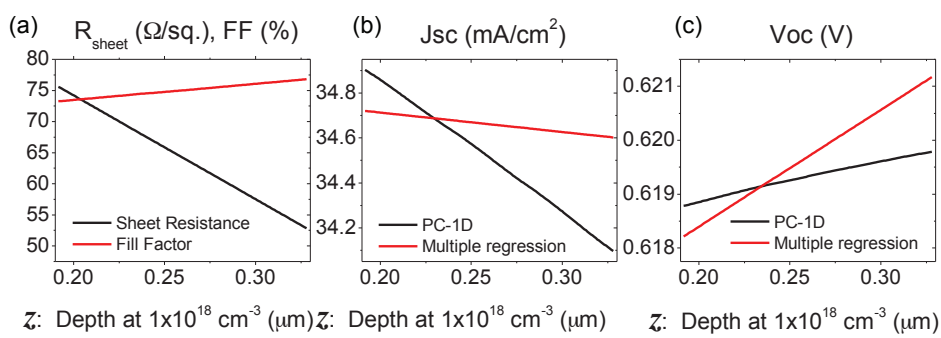

Fig. 5. Calculated dependences upon z (depth at $N_P = 1\times10^{18}$ /cm³) by multiple regression analysis and PC1D with employing the peak N_P (= x) as 7.8×10^{20} /cm³ and the depth at $N_P = 5\times10^{19}$ /cm³ (= y) as 0.076 µm. (a) R_{sheet} and *FF*, (b) J_{sc}, and (c) V_{oc}.

Fig. 5(b) shows the trend of J_{sc} calculated with the multiple regression analysis compared to the PC1D output. Both show decreasing J_{sc} with the increasing n^+ depth, suggesting that the contribution to the photo-generated current of the emitter layer is smaller than that of the base layer if they are located at the same depth from the surface. But the inclination of our regression model is much smaller than in PC1D, which may be caused by the imperfect simulation of the surface texture using PC1D.

The V_{oc} trend shown in Fig. 5(c) is more interesting. As described in section 3.2, a deeper n^+ contributes to higher V_{oc}, an effect of which is supported by our regression analysis [6]. Presumably, it is caused by the difference in the impact of Auger recombination between the n^{++} and n^+ layers. Due to the current continuity principle, I_{0e} of the whole emitter is limited by either the n^{++} or the n^+, depending on which local value of I_{0e} is lower. Because of the presence of more Auger recombination centers in the n^{++} and less in the n^+ regions, the I_{0e} of the n^+ decreases with increasing depth due to relatively fewer thermally equilibrated holes, and becomes lower than that of the n^{++}, resulting in the increase in V_{oc}. The PC1D output suggests this presumption by showing the increase in V_{oc} with increasing the n^+ depth, under its consideration on Auger recombination, although the inclination of the PC1D output is smaller than the result of our regression analysis.

5. Conclusions

We designed a process to control the n^{++} and n^+ layers independently in a uniform emitter without increasing the total process time or including extra process steps. By manipulating the doping profile, we achieved an increase in both J_{sc}*V_{oc} and *FF* simultaneously while maintaining or increasing the process window for the Ag contacting process. Improving the doping profile by increasing the depth of the n^+ layer and reducing the peak N_P resulted in an efficiency gain of $0.3\%_{abs}$. The obtained sheet resistance was as low as 51-56 ohm/square, compared to the 66 ohm/square of the conventional process. The doping profile of the n^{++} layer enables a sufficiently large tolerance for the Ag paste to penetrate, yielding low contact resistance. The cause of the contribution of the deeper n^+ layer to higher V_{oc} has been analyzed using statistical multiple regressions and PC1D simulation. The results suggest that I_{0e} decreases with the deeper n^+ layer because of less Auger recombination centers in n^+ while more in n^{++}. This creates the lower I_{0e} in the n^+ than in the n^{++}, which limits the I_{0e} of the whole emitter, and causes the decrease in I_{0e} with increasing the depth of the n^+.

Acknowledgements

Part of this work was financially supported by the AgentschapNL EOS-KT program DEEP, nr IS074007.

References

[1] Bentzen A, Holt A, Christensen JS, Svensson BG, *J. Appl. Phys.*, 2006, **99**, 064502.
[2] Slotboom JW, de Graaff HC, *Solid-State Electronics*, 1976, **19**, 857-62.
[3] Tyagi MS, van Overstraeten R, *Solid-State Electronics*, 1983, **26**, 577-97
[4] Komatsu Y, Galbiati G, Lamers M, et al., *24th EU-Photovoltaic Solar Energy Conference*, Hamburg 2009, 1063-7.
[5] Sze SM, *Physics of Semiconductor Devices*, John Wiley & Sons, 2nd ed., New York, 1981.
[6] Komatsu Y, Stassen AF, Venema PR, et al., *25th EU-Photovoltaic Solar Energy Conference*, Valencia 2010, 1924-9.
[7] Schubert G, Huster F, Fath P, *19th EU-Photovoltaic Solar Energy Conference*, Paris 2004, pp. 813-6.
[8] PC1D Version 5.9, http://www.pv.unsw.edu.au/links/products/pc1d.asp